https://doi.org/10.2352/ISSN.2470-1173.2019.14.COLOR-083
© 2019, Society for Imaging Science and Technology

Viewing angle characterization of HDR/WCG displays using color volumes and new color spaces

Pierre Boher and Thierry Leroux, ELDIM, 1185 rue d'Epron, 14200 Hérouville St Clair, France
Pierre Blanc, Laboratoires d'Essai de la FNAC, 2 rue des Champarts, 91742 Massy, France

Abstract

Color volumes in the new color spaces IC_tC_p and $J_za_zb_z$ are used to characterize the performances of different types of displays. The viewing angle behavior of the emissive properties of one QLED TV and one OLED TVs are measured and compared. The influence of the top polarizer on the reflective properties of one LCD vehicle display is also measured and the color performances under various parasitic illumination are predicted.

Introduction

Many high dynamic range (HDR) and wide color gamut (WCG) displays made with different technologies are now commercially available and adapted methods to characterize their color and reflective properties are required. Concerning the color properties, the gamut is very restrictive because it does not involve the luminance range. On the contrary color volume involving both color gamut and luminance is a much better descriptor for the color properties. We have proposed to use color volumes to analyze viewing angle color measurements on displays several years ago [1-3]. In these earlier studies, the standard L*a*b* CIE 1976 and L*u*v* color spaces have been used. The international committee for display metrology has also standardized the method [4]. More recently we have introduced new color spaces especially developed for HDR and WCG contents and in particular the IC_tC_p color space recently proposed by Dolby laboratories [5] or the $J_za_zb_z$ color space [6] to do the same task [7-10].

Characterization of the emissive properties is not enough for several practical applications because parasitic light always plays a role in the performances. We have already proposed to use the spectral BRDF of each display surface to predict its performances under illumination conditions [11-13]. In this respect, color volume can also be used to quantify the color properties of displays under parasitic illumination.

In the following, we use viewing angle measurements made on different displays both in emissive and reflective configuration to quantify their color properties using IC_tC_p and $J_za_zb_z$ color volumes. Emissive properties of one QLED TV and one OLED TV, and the influence of the top polarizer of an LCD automotive display are presented at examples of application.

Experimental techniques

Multispectral viewing angle measurements

The first Fourier optics viewing angle measurement system was first publicly introduced by ELDIM at Eurodisplay'1993 [14]. The Fourier optic is designed in order to convert angular field map into a planar one allowing very rapid measurements of the full viewing cone. Each light beam emitted by the sample surface is collected by the optics and refocus on a Fourier plane at a position proportional to the incidence and azimuth angles (cf. figure 1). This Fourier plane is reimaged on a CCD detector. The multispectral system EZContrastMS measures the full viewing angle up to 88° versus wavelength using to 31 band-pass filters regularly distributed in the visible range every 10nm [15].

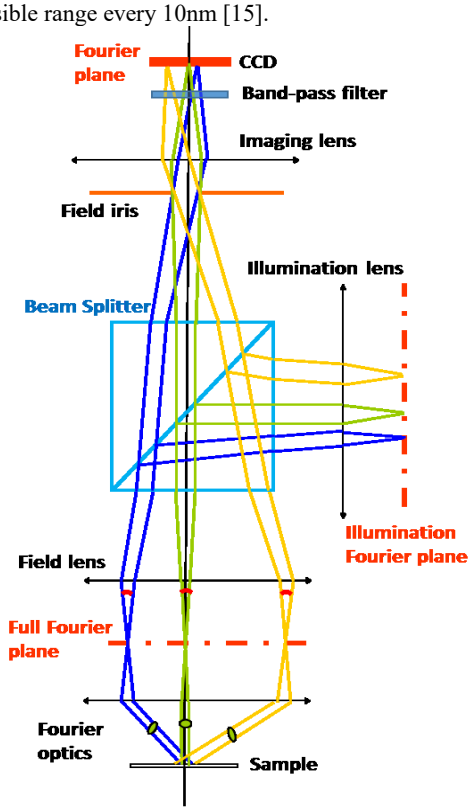

Figure 1. Schematic diagram of a Fourier optics system with beam splitter for internal illumination

Reflective measurements

For reflective measurements, it is necessary to illuminate the sample. It is made using a beam splitter and an additional optics that allows illumination at all the angles easily and accurately (cf. figure 1). An illumination lens reimages the first Fourier plane on an illumination plane. One point on this plane corresponds to one incidence on the surface of the sample. This instrument is classically used to perform spectral BRDF measurements on isotropic [16] or anisotropic surfaces [17].

Full diffused reflectance

The full diffused reflectance $R(\theta_o, \varphi_o, \lambda)$ depends on two observation angles θ_o and φ_o and the wavelength λ, as shown in figure 2.a and the following formula:

$$R(\theta_o, \varphi_o, \lambda) = \frac{L_s(\theta_o, \varphi_o, \lambda) - L_{trap}(\theta_o, \varphi_o, \lambda)}{L_{glass}(\theta_o, \varphi_o, \lambda) - L_{trap}(\theta_o, \varphi_o, \lambda)} R_{glass}(\theta_o, \lambda)$$

(θ_o,φ_o) are the polar coordinates of the observation direction, L_s, L_{glass} and L_{trap} are the radiance measured on the sample, one black glass and a light trap in the same illumination conditions. We use a black glass as reference sample since its reflectance depends only on its optical index and can be computed versus angle and wavelength $R_{glass}(\theta_o,\lambda)$. A white reference sample can be also used but its reflectance at high angle is not perfectly known. The illumination is made with an integration sphere whose exit is located on the illumination Fourier plane (cf. figure 1). The parasitic internal reflections are partially corrected using a measurement on a light trap with the same illumination conditions.

Collimated beam BRDF

Collimated beam illumination is realized with an optical fiber located on the illumination plane and moved to change the incidence and azimuth of the beam (cf. figure 1). The spectral BRDF depends on two incidence angles θ_i and φ_i, two observation angles θ_o and φ_o and the wavelength λ, as shown in figure 2.b. It is given by the following formula:

$$BRDF(\theta_i,\varphi_i,\theta_o,\varphi_o,\lambda)=\frac{L_s(\theta_o,\varphi_o,\lambda)}{E_i(\theta_i,\varphi_i,\lambda)}$$

The luminance L_s is directly given by the Fourier optics measurement on the sample. The irradiance of the incident beam E_i is evaluated by the integration a white reference measurement in the same illumination conditions.

$$E_i(\theta_i,\varphi_i,\lambda)=\iint_{2\pi} R_w(\theta_o,\lambda)\,L_W(\theta_o,\varphi_o,\lambda)\cos(\theta_o)\,d\omega_o$$

$R_w(\theta_o,\lambda)$ is the reflectance of a white reference sample.

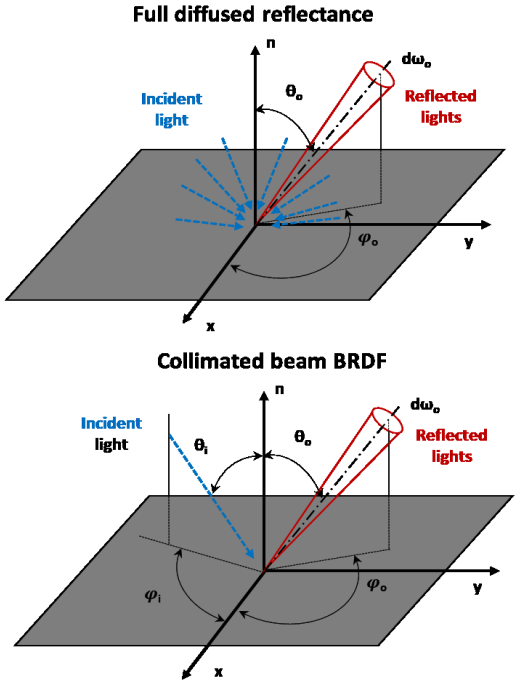

Figure 2 . Definition of the full diffused reflectance (top) and the spectral BRDF (bottom)

Color analysis:

IC_tC_p and $J_zA_zB_z$ color spaces have been recently introduced to offer a space perceptually uniform over a wide gamut, linear in iso-hue directions and to be efficient to predict both small and large color differences. IC_tC_p has been introduced by Dolby laboratories in order to match the new video format for HDR/WCG video compression [5]. The transformation from XYZ CIE components to IC_tC_p space consists in three successive operations; conversion to three cones human response space LMS; nonlinear conversion to adjust dynamic range and color differencing equations.

$$\begin{pmatrix}L\\M\\S\end{pmatrix}=\begin{pmatrix}0.3592 & 0.6976 & -0.0358\\ -0.1922 & 1.1004 & 0.0755\\ 0.0070 & 0.0749 & 0.8434\end{pmatrix}\begin{pmatrix}X\\Y\\Z\end{pmatrix}$$

$$L'M'S'=EOTF_{PQ}^{-1}(LMS)$$

$$\begin{pmatrix}I\\Ct\\Cp\end{pmatrix}=\begin{pmatrix}0.5 & 0.5 & 0\\ 1.6137 & -3.3234 & 1.7097\\ 4.3780 & -4.2455 & -0.1325\end{pmatrix}\begin{pmatrix}L'\\Y\\Z\end{pmatrix}$$

$J_zA_zB_z$ color space has been built in the same way with two additional operations, green-blue adjustment on XYZ CIE components, conversion to three cones human response space LMS; nonlinear conversion to adjust dynamic range, color differencing equations and lightness J_z computation [16].

$$\begin{bmatrix}X'\\Y'\end{bmatrix}=\begin{bmatrix}bX\\gY\end{bmatrix}-\begin{bmatrix}(b-1)Z\\(g-1)X\end{bmatrix}$$

$$\begin{pmatrix}L\\M\\S\end{pmatrix}=\begin{pmatrix}0.4147 & 0.5799 & 0.0146\\ -0.2015 & 1.1206 & 0.0531\\ 0.0166 & 0.2648 & 0.6684\end{pmatrix}\begin{pmatrix}X'\\Y'\\Z\end{pmatrix}$$

$$L'M'S'=EOTF'^{-1}_{PQ}(LMS)$$

$$\begin{pmatrix}Iz\\az\\bz\end{pmatrix}=\begin{pmatrix}0.5 & 0.5 & 0\\ 3.524 & -4.066 & 0.542\\ 0.199 & 1.096 & -1.295\end{pmatrix}\begin{pmatrix}L'\\Y\\Z\end{pmatrix}$$

$$Jz=\frac{(1+d)Iz}{1+dIz}$$

The Electro-Optical Transfer Function EOTF^{-1} is designed to match the contrast sensitivity function of the human eye [17].

$$EOTF^{-1}(X)=\left(\frac{C_1+C_2X^{m1}}{1+C_3X^{m1}}\right)^{m2}$$

X is the luminance level normalized between 0 and 1 using a reference luminance level (100, 1000 or 10000cd/m^2 depending on the application). The shape of the EOTF^{-1} function is given in figure 3 showing the reduction of sensitivity of the human eye for the low luminance levels.

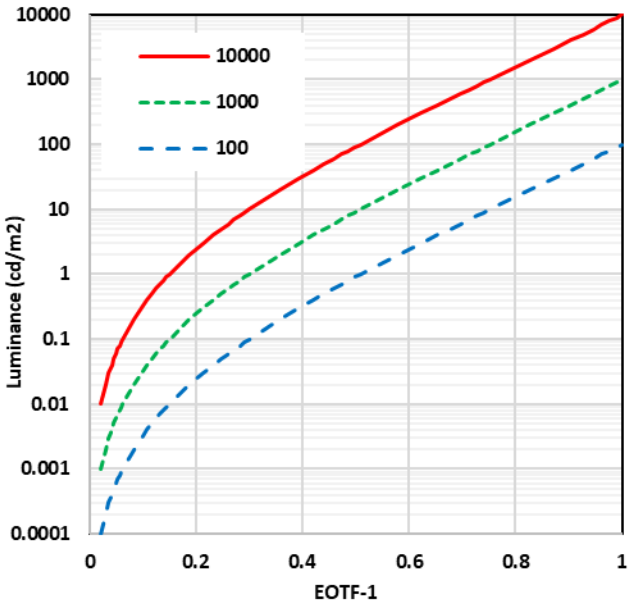

Figure 3 . Inverse of the Electro-optical transfer function EOTF^{-1} computed for different luminance reference levels.

Experimental results

QLED and OLED TVs

The color viewing angle of one QLED TV (Samsung QE49Q7AMT) and one OLED TV (LG OLED65C7V) have been measured for the white, black, red, green, blue, magenta, cyan and yellow states. The color volume at each angle in the XYZ color space is a polyhedron that can be directly deduced from the coordinates of these different states since this space is completely linear.

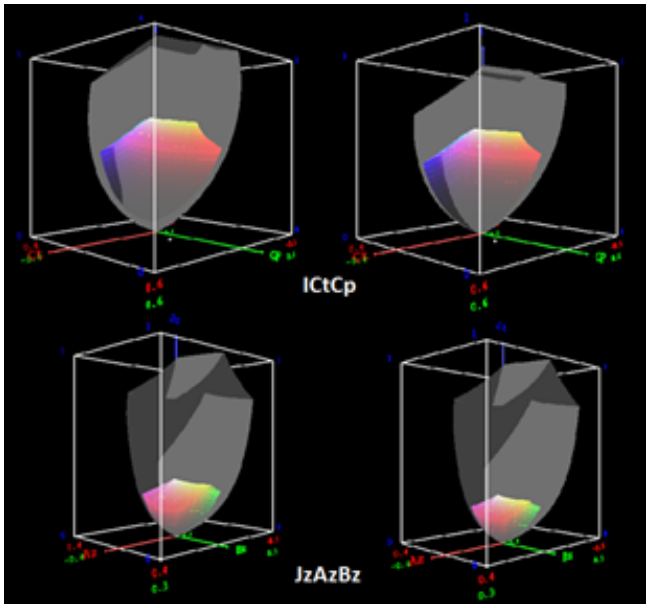

Figure 4 . Color volume at normal incidence of the QLED TV (left) and OLED TV (right) in the IC_tC_p (top) and $J_za_zb_z$ (bottom) color spaces.

A conversion to the other color spaces gives the different color volume as shown in figure 4 where the color volumes computed in the two color spaces at normal incidence on the QLED and OLED TVs are reported. The Rec2020 reference volume is also reported in gray in the same figure. The Rec2020 reference volume is computed for a white luminance value of 10000cd/m^2 and can be compared directly to the volume of the two displays. We see immediately that the two displays suffer from an intensity level much lower than the Rec.2020 reference for all the colors and that the color volumes of the two displays are quite comparable at normal incidence even if there are much smaller than Rec.2020 reference. The difference is amplified for the $J_za_zb_z$ color space because of the different perceptual OETF function.

The angular behavior of the volume ratio to Rec2020 reference volume for the two displays is also reported in figure 5. The two displays have comparable volumes at normal incidence but the QLED display shows a strong decrease of the volume ratio at high angles for all the color spaces. The decrease is more moderated for the OLED display ensuring better properties at oblique angles than the QLED display.

To compare more easily the two displays we have also computed the angular behavior of the IC_tC_p color volume gravity center. Angular behaviors of the color coordinates C_t and C_p of the two displays with the same scales are reported in figure 6. The global color shift is slightly different for the two displays. A more important red shift can be seen for the QLED display at normal incidence. In addition, the angular dependence is very different for the two displays. The OLED display is more efficient in terms of color because it maintains a high color volume in the entire viewing angle and the color properties are more stable than those of the QLED display.

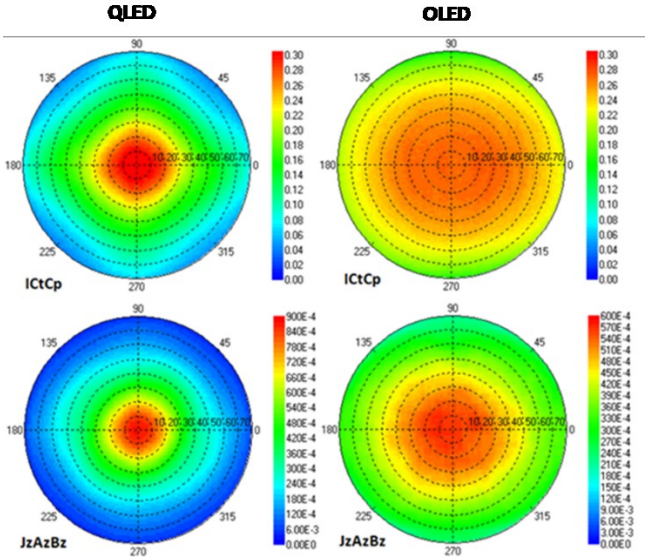

Figure 5 . Color Volume ratios to Rec.2020 of QLED (left) and OLED (right) TVs versus angles using the IC_tC_p (top) and $J_za_zb_z$ (bottom) color spaces.

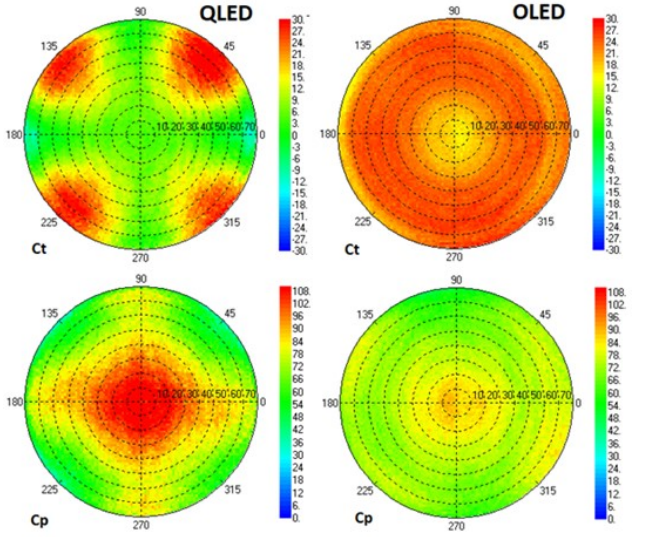

Figure 6 . Color coordinates of the IC_tC_p volume gravity center of QLED (left) and OLED (right) TVs versus angles

Vehicle LCD display with different top polarizers

The top polarizer of one automotive LCD display has been replaced by four different polarizer films on the four quarters of the display surface: one anti-glare low reflection polarizer (AGLR), one anti-glare anti-reflection polarizer (AGAR) and two anti-glare polarizers (AG30) and (AG380). The emissive properties of LCD display with the four top polarizers are very similar. The impact of the polarizers takes place essentially on the reflective properties.

Reflective properties

The reflective properties of the four quarters of the display have been measured in full diffused illumination while switched off. The angular dependence of the spectral reflectance is isotropic with a

shape similar to a glass/air interface but with very different levels depending on the type of polarizer (cf. figure 6). The AG30 and AG380 polarizers give similar results with a reflectance level near 5% at normal incidence (cf. figure 6). The AGAR polarizer exhibits a much lower reflectance coefficient less than 1% at normal incidence. The AGLR polarizer is intermediate between these values.

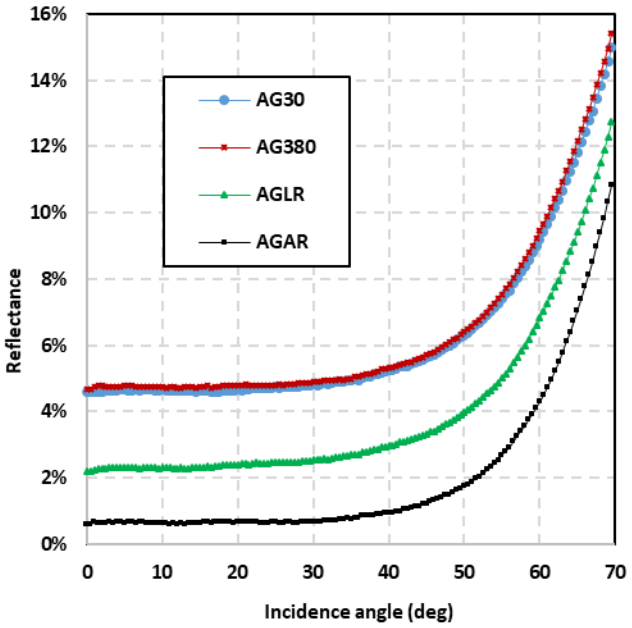

Figure 6 . Full diffused reflectance of a vehicle display with 4 top polarizers at 600nm versus incidence angle.

The spectral BRDF of the four polarizers on top of the LCD display have been measured for a fixed incidence angle of 25°.The four angular patterns obtained at a wavelength of 600nm are reported in figure 7 with the same logarithmic scale. In each case, a specular reflection is observed with a haze component that is more or less extended in angle depending on the type of polarizer. The specular component is low for the AGLR and AGAR polarizers in agreement with the observed full diffused reflectance (cf. figure 6). AG30 and AG380 polarizers show a high specular reflectance and different haze component. AG320 is much glossier than AG30. AGAR shows a very low BRDF and a more mirror like behavior in agreement with results obtained in full diffused illumination. AGLR is intermediate.

Performances under illumination

To evaluate the performances under illumination, we compute the CIE components X, Y, Z of the white, black, red, green, blue, cyan, magenta and yellow states with additional full diffused or collimated beam illumination using:

$$Y(\theta,\varphi) = Y_i(\theta,\varphi) + \int L(\lambda)R(\theta,\varphi,\lambda)y_{CIE}(\lambda)d\lambda$$

$$Y(\theta_i,\varphi_i,\theta,\varphi) = Y_i(\theta,\varphi) + \int R(\lambda)BRDF(\theta_i,\varphi_i,\theta,\varphi,\lambda)y_{CIE}(\lambda)d\lambda$$

The integration is made in the visible range. R(θ,φ,λ) is the full diffused spectral reflectance and BRDF$(\theta_i,\varphi_i,\theta,\varphi,\lambda)$ is the collimated beam BRDF. $Y_i(\theta,\varphi)$ is the intrinsic emissive properties for each CIE component, $y_{CIE}(\lambda)$ the corresponding CIE function, and L(λ) and R(λ) the spectral radiance of the external illumination. In the following all the simulations are made with a D65 illuminant with variable level.

.

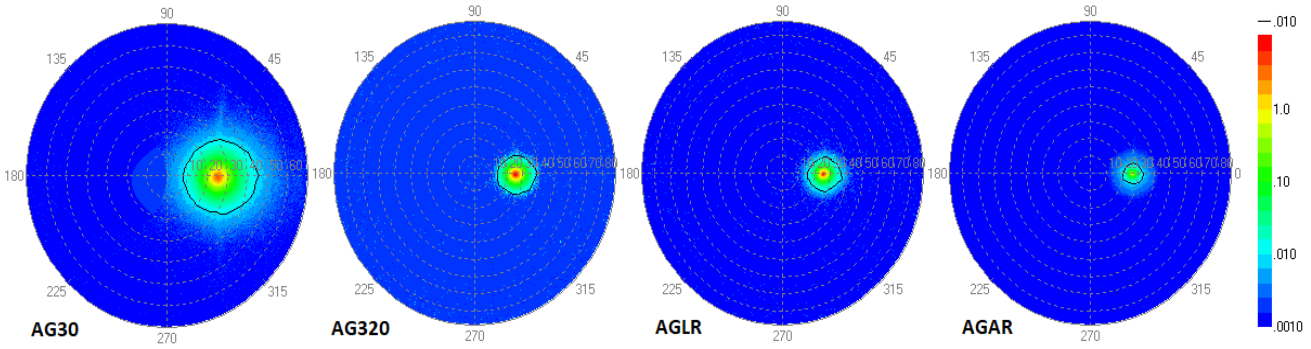

Figure 7 .BRDF measured at 600nm of the LCD display with the four top polarizers: isovalue at 0.01str^{-1} is reported.

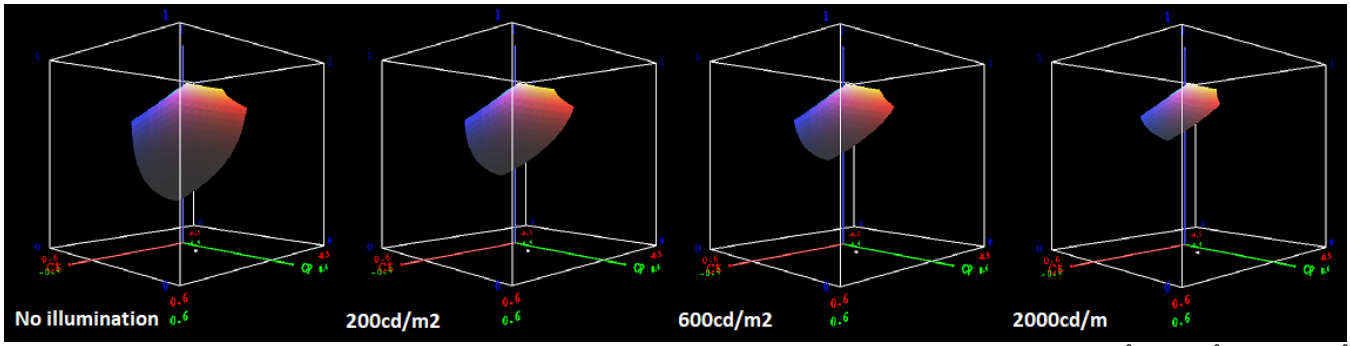

Figure 8 . color volume computed in the IC_tC_p space of the LCD AGAR polarizer at normal incidence without illumination and with 200cd/m^2, 600cd/m^2 and 2000cd/m^2 full diffused illumination.

On figure 8 we have reported the IC_tC_p color volumes of the LCD with AGAR polarizer without illumination and with a full diffused external illumination of 200, 600 and 2000cd/m^2. The reduction of the color volume is important even for a low-level parasitic illumination. The shrinkage of the low part of the color volume along the intensity axis is due to a higher impact on the low color levels and to the non-linearity of the EOTF^{-1} function (cf. figure 3). The color volume ratio to sRGB at normal incidence computed in the IC_tC_p color space versus the full diffused illumination is reported in figure 9 for the four polarizers. The two antiglare polarizers give comparable results. The AGAR polarizer gives the best performances under full diffused illumination.

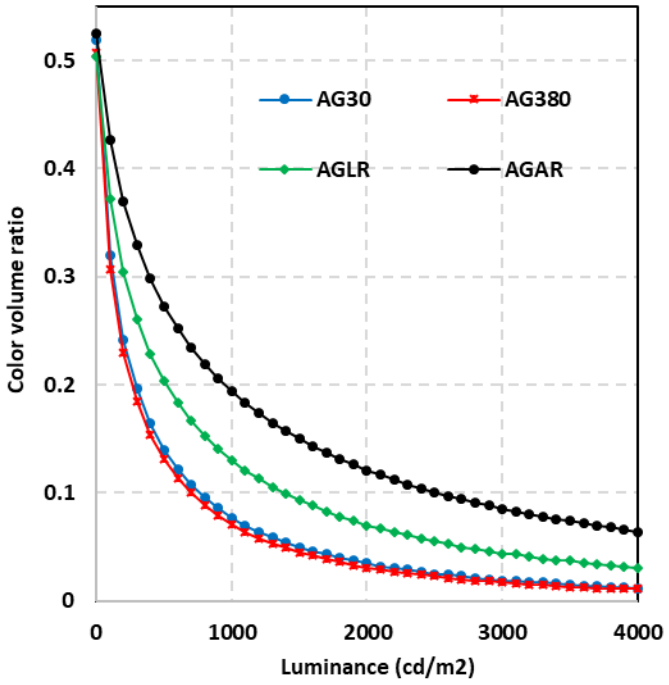

Figure 9 . Color volume ratio to sRGB in the IC_tC_p space at normal incidence versus full diffused illumination external luminance

The same type of simulation has been performed for a collimated beam of incidence 25° using the spectral BRDF measurements. The color volume ratio to sRGB at 20° of incidence near the specular reflection computed in the IC_tC_p color space versus the illumination level is reported in figure 10 for the four polarizers. In these conditions, the two antiglare polarizers AG30 and AG320 give now very different results due their different glossy aspects (cf. figure 7). It is then useful to perform reflective measurements in full diffused and collimated beam illumination conditions which are two limit cases: full diffused illumination gives an overall idea of the reflection power of the surface without any influence of the gloss properties, when collimated beam illumination emphasize the role of the gloss. Both conditions are required to test the display performances under external illumination. Anyway, the AGAR polarizer stays the best candidate in the two illumination conditions.

To compare more efficiently the color volume analysis method to standard methods like luminance contrast and color gamut, we have summarized different results obtained with the three methods and for the two illumination conditions on the four top polarizers in table 1. The analysis of the luminance contrast reduction under any illumination gives strongest reduction in all the cases. This strong reduction is not directly linked to the human sensation since optical response of the human eye is not linear. On the contrary the color gamut analysis is always quite optimistic but does not take into account the luminance reduction. The color volume analysis which includes both properties together is certainly the best parameter available to compare the different samples and to analyze their performances with and without external illumination.

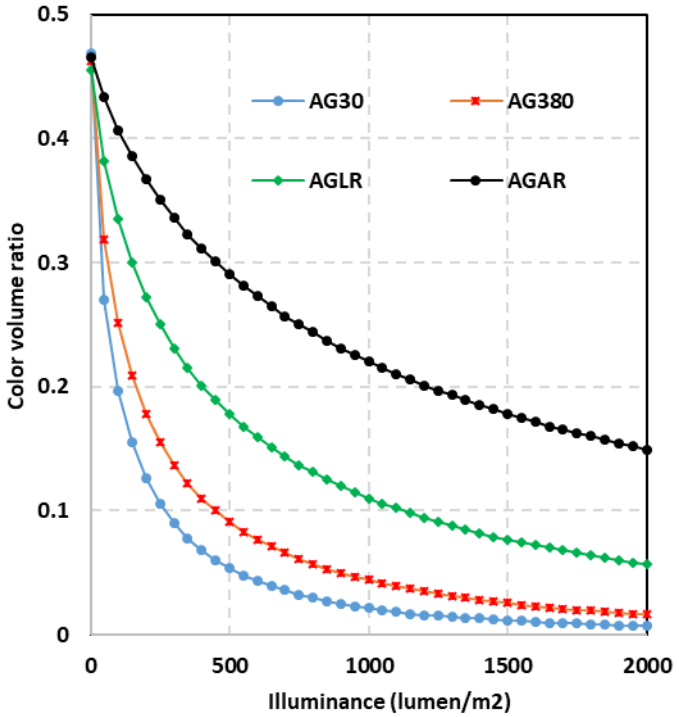

Figure 10 . Color volume ratio to sRGB in the IC_tC_p space at 20° of incidence versus collimated beam illumination at 25°.

Conclusions

High dynamic range (HDR) and wide color gamut (WCG) displays require adapted color analysis to extract reliable color characteristics and compare efficiently the displays. The new IC_tC_p and $J_za_zb_z$ color spaces have been defined specifically for this kind of displays. So, it is logical to use them to analyze color measurements on such displays. It is what we propose in this paper using color viewing angle measurements made with our Fourier optics systems. The analysis using the IC_tC_p and $J_za_zb_z$ color spaces is really innovative and interesting and can be also applied to all types of displays and not only HDR/WCG displays.

The analyzis of the influence of the top polarizer of a vehicle display is another interesting example. In this case, the intrinsic emissive properties are not sufficient to compare the performances that are most of the time affected by the parasitic light. Reflective properties of vehicle displays must be also taken into account and multispectral Fourier optics viewing angle instruments are very well adapted to study this type of problem because of their capacity to make high resolution reflective angular measurements rapidly and with different illumination configurations. Measurements using different illumination configurations are helpful to understand better the reflective properties of such displays and to select the best candidate for practical use. Full diffused illumination conditions are useful to get an overall overview of the reflection properties but do not distinguish between surfaces with different gloss on the contrary of the BRDF measurements. It has been clearly demonstrated on the experimental results reported prevously with the two antiglare polarizers that show comparable full diffused reflectance properties but very different glossy surfaces. Color analysis must be made in the two conditions to compare efficiently the different solutions. Spectral BRDF measurements have also an additional interest because there can be used to make physico-realistic simulations with complex illumination configurations as presented in another talk of the same conference [18].

Table 1: summary of the properties of the different top polarizers on the LCD display with two different parasitic illumination conditions. Luminance contrast, color gamut and color volume in the IC_tC_p color space are reported

Top Polarizer	Emissive properties			Under Full diffused illumination			Reduction ratio		
	observation on axis			*2000cd/m², observation on axis*			*observation on axis*		
	Luminance contrast	Color gamut	Volume ratio to sRGB	Luminance contrast	Color gamut	Volume ratio to sRGB	Luminance contrast	Color gamut	Volume ratio to sRGB
AG30	596.4	0.701	51.9%	5.4	0.222	3.5%	0.90%	31.67%	6.74%
AG380	616.4	0.695	50.7%	5.2	0.200	3.1%	0.84%	28.80%	6.11%
AGLR	566.0	0.709	50.4%	9.1	0.351	7.0%	1.61%	49.53%	13.89%
AGAR	930.5	0.703	52.5%	19.9	0.476	12.1%	2.14%	67.71%	23.05%
Top Polarizer	**Emissive properties**			**Under collimated beam illumination**			**Reduction ratio**		
	observation 20°			*2000cd/m² at 25°, observation 20°*			*observation 20°*		
	Luminance contrast	Color gamut	Volume ratio to sRGB	Luminance contrast	Color gamut	Volume ratio to sRGB	Luminance contrast	Color gamut	Volume ratio to sRGB
AG30	371.5	0.698	46.9%	17.8	0.067	0.7%	4.80%	9.65%	1.49%
AG380	399.3	0.692	46.2%	52.9	0.093	1.7%	13.25%	13.38%	3.68%
AGLR	357.1	0.695	45.5%	59.4	0.292	5.7%	16.62%	41.98%	12.53%
AGAR	511.6	0.698	46.5%	100.6	0.541	14.9%	19.66%	77.51%	32.04%

References

[1] P. Boher, T. Leroux, T. Bignon, V. Collomb-Patton, "A new method to evaluate the viewing angle color performances of displays", IDMC, Taipei, Taiwan, April (2011)

[2] P. Boher, T. Leroux, T. Bignon, P. Blanc, "Color display evaluation vs. viewing angle using L∗a∗b∗ color space and Fourier-optics measurements", J. of Information Display, Vol. 12, N°4, 179 (2011)

[3] P. Boher, T. Leroux, T. Bignon, V. Collomb-Patton, "Precise Evaluation of the Colorimetric Properties of Displays SID, 70.3 (2011).

[4] "Information Display Measurements Standard (IDMS), 5.31 Volume color reproduction capability", IDMS V.1.03 (2012)

[5] T. Lu, F. Pu, P. Yin, T. Chen, W. Husak, J. Pytlarz, R. Atkins, J. Hlich, G. Su., "ITP Color space and its compression performance for high dynamic range and wide color gamut video distribution", ZTE Communications, Feb., Vol.14, N°1 (2016)

[6] M. Safdar, G. Cui, Y. Kim, M. Ronnier Luo, "Perceptually uniform color space for image signals including high dynamic range and wide gamut", Optics Express, Vol. 25, N°13, 15131 (2017)

[7] P. Boher, T. Leroux, P. Blanc, "Viewing angle color evaluation of QLED and OLED HDR displays using Lab and ICtCp color spaces", IDW, Sendai, Japan, December (2017)

[8] P. Boher, T. Leroux, P. Blanc, "New ICtCp and Jzazbz Color Spaces to Analyze the Color Viewing-Angle Dependence of HDR and WCG Displays", Display Week, Los Angeles (2018)

[9] P. Boher, T. Leroux, P. Blanc, "Optical characterization of the emissive properties of HDR/WCG displays using ICtCp color space and Fourier optics viewing angle instruments", Electronic Imaging Conference, San Francisco, USA, January (2018)

[10] P. Boher, T. Leroux, P. Blanc, "New ICtCp and Jzazbz Color Spaces to Analyze the Color Viewing-Angle Dependence of HDR and WCG Displays", Display Week, Los Angeles (2018)

[11] P. Boher, T. Leroux, T. Bignon, V. Leroux, "Optical measurements for comparison of displays under ambient illumination and simulation of physico-realistic rendering", Vehicle Displays Symposium, Dearborn, Michigan, October 20-21 (2011)

[12] P. Boher, T. Leroux, V. Collomb-Patton, V. Leroux, "Physico-realistic simulation of displays", Vehicle Displays Symposium, Dearborn, October 18-19 (2012)

[13] P. Boher, T. Leroux, V. Leroux, E. Sandré-Chardonnal, "Physico-realistic ray tracing simulation of displays under indoor or outdoor illumination", Vehicle Displays Symposium, Dearborn, Michigan, October 22-23 (2015)

[14] T. Leroux, "Fast contrast vs. viewing angle measurements for LCDs," 13th Int. Display Research Conf., 447 (1993)

[15] P. Boher, T. Bignon, T. Leroux, D. Glinel, "New multispectral Fourier optics viewing angle instrument", SID, P.89 (2008)

[16] P. Boher, T. Leroux, V. Collomb-Patton, T. Bignon, "New generation of Fourier optics instruments for fast multispectral BRDF characterization", SPIE Imaging, 9398, 16 (2015)

[17] P. Boher, T. Leroux, T. Bignon, V. Collomb-Patton, "Multispectral BRDF measurements on anisotropic samples: application to metallic surfaces and OLED displays", IS&T International Symp. On Electronic Materials, MMRMA-359(2016

[18] P. Boher, T. Leroux, T. Muller, P. Porral, "Accurate physico-realistic ray tracing simulation of displays", Electronic Imaging, Material Appearance Conference (2019)

Author Biography

Pierre Boher earned an Engineer degree at ECP, "Ecole Centrale des Arts et Manufactures" in 1982. He obtained his Ph.D. in material sciences in 1984 and his ability to research management at "University Pierre et Marie Curie" in 1991. He worked in the French Philips Laboratories during nine years on the deposition and characterization of very thin films and multilayers. R&D manager at SOPRA between 1995 and 2002, he developed different metrology tools for non-destructive characterization mainly for microelectronics. He joined ELDIM as R&D manager in 2003.

JOIN US AT THE NEXT EI!

IS&T International Symposium on

Electronic Imaging

SCIENCE AND TECHNOLOGY

Imaging across applications . . . Where industry and academia meet!

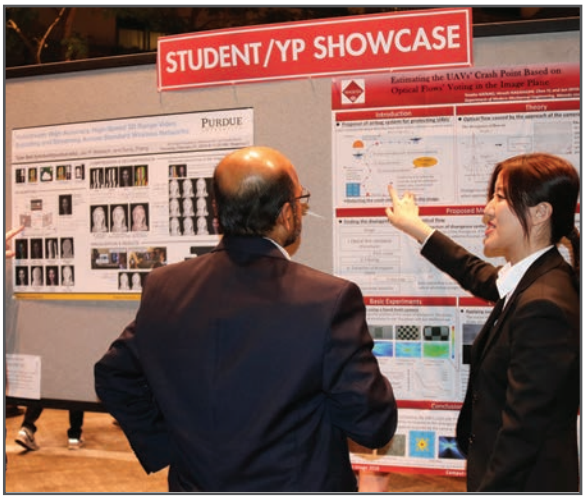

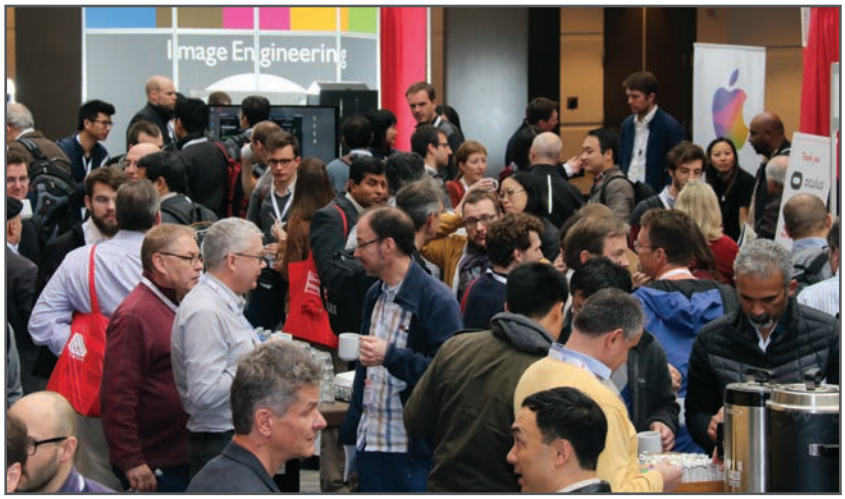

• SHORT COURSES • EXHIBITS • DEMONSTRATION SESSION • PLENARY TALKS •
• INTERACTIVE PAPER SESSION • SPECIAL EVENTS • TECHNICAL SESSIONS •

www.electronicimaging.org

IS&T
imaging.org